



Initial results from electron microscopy from AGR 5/6/7 Capsule 1 fuel and

July 2023

Changing the World's Energy Future

Lu Cai



DISCLAIMER

This information was prepared as an account of work sponsored by an agency of the U.S. Government. Neither the U.S. Government nor any agency thereof, nor any of their employees, makes any warranty, expressed or implied, or assumes any legal liability or responsibility for the accuracy, completeness, or usefulness, of any information, apparatus, product, or process disclosed, or represents that its use would not infringe privately owned rights. References herein to any specific commercial product, process, or service by trade name, trade mark, manufacturer, or otherwise, does not necessarily constitute or imply its endorsement, recommendation, or favoring by the U.S. Government or any agency thereof. The views and opinions of authors expressed herein do not necessarily state or reflect those of the U.S. Government or any agency thereof.

Initial results from electron microscopy from AGR 5/6/7 Capsule 1 fuel and

Lu Cai

July 2023

**Idaho National Laboratory
Idaho Falls, Idaho 83415**

<http://www.inl.gov>

**Prepared for the
U.S. Department of Energy
Under DOE Idaho Operations Office
Contract DE-AC07-05ID14517**

July 25, 2023

Lu Cai, Ph.D.

Nuclear Engineer

Idaho National Laboratory

Initial results from electron microscopy from AGR-5/6/7 Capsule 1 fuel and applications of other microanalysis techniques to irradiated TRISO fuel

DOE ART Gas-Cooled Reactor (GCR) Review Meeting

Virtual Meeting

July 25 – 27, 2023





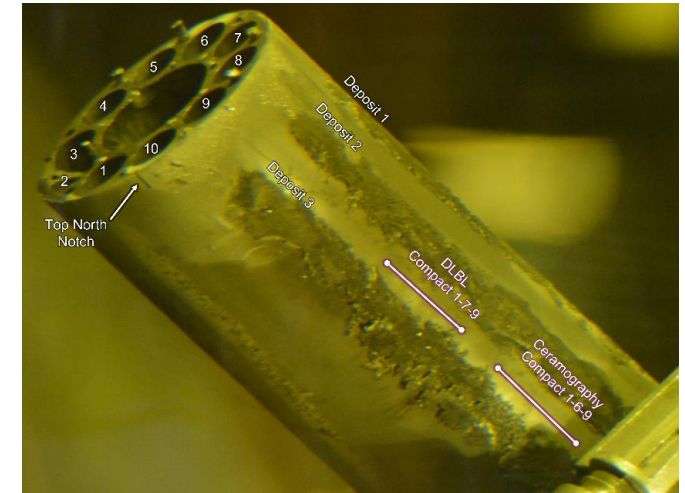
Outline

- Characterization of particles from AGR-5/6/7 Capsule 1
 - Background and Motivation
 - X-ray computed tomography on four particles from Compact 1-7-9
 - SEM/EDS of particles from Compacts 1-7-9 and 1-7-4
 - Summary
- Local Thermal Conductivity Measurement on AGR-2 particles

Characterization of Particles from AGR-5/6/7 Capsule 1

Background and Motivation – Capsule 1

- AGR-5/6/7 Capsule 1 had significant rates of in-pile TRISO fuel particle failure, likely caused by Ni from thermocouples reacting with SiC layers.
- Four randomly-selected particles from Compact 1-7-9 were examined with x-ray tomography for signs of coating degradation and evidence of nickel attack.
- A few particles from Compacts 1-7-9 and 1-7-4 were investigated by scanning electron microscope (SEM) to compare the microstructure and to look for evidence of nickel in the fuel



Ref: INL/RPT-22-66720, "Initial Observations from AGR 5/6/7 Capsule 1."

Characterization of Particles from AGR-5/6/7 Capsule 1 X-ray Computed Tomography

Collaborators:

John D. Stempien

Joshua J. Kane

Rahul Reddy Kancharla

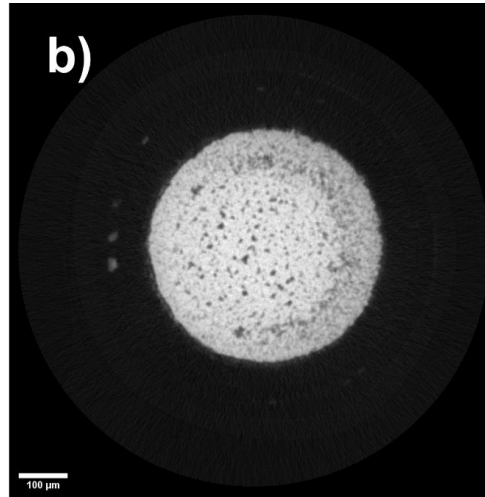
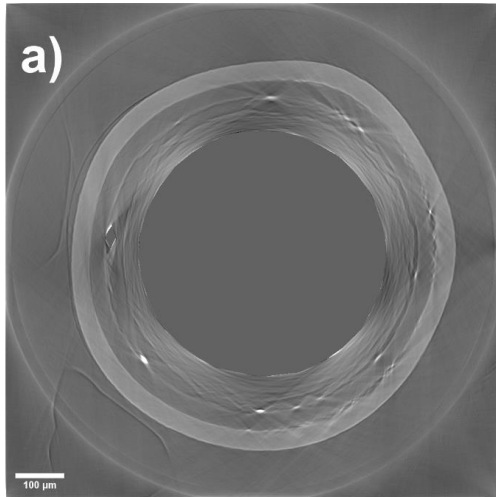
William C. Chuirazzi

Miles T. Cook

Quintin D. Harris

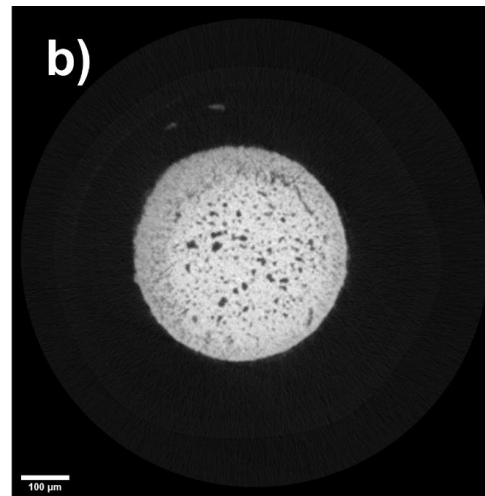
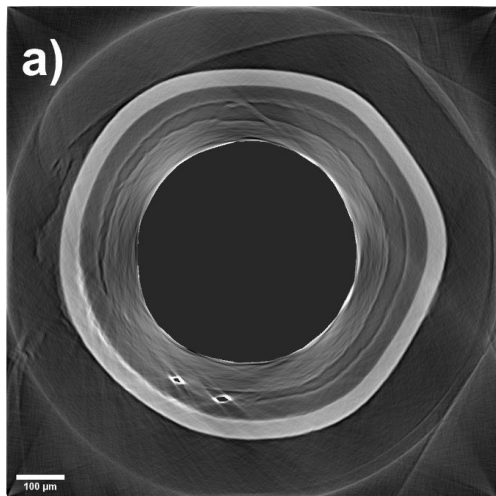
XCT- Particles A, C, and D

Particle A

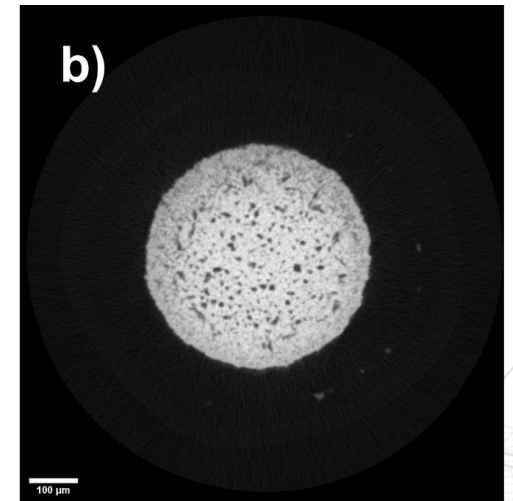
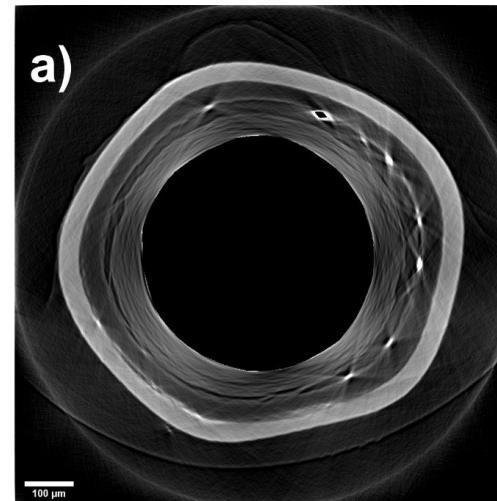


- Low energy (a) and high energy (b) XCT scans through the particle center
- Each of three particles particle has an intact SiC layer.
- The IPyC layers appear well adhered to the SiC layer.
- The IPyC and buffer layers appear to have separated over the majority of the volume of each particle.
- A number of dense features are observed within the TRISO layers.

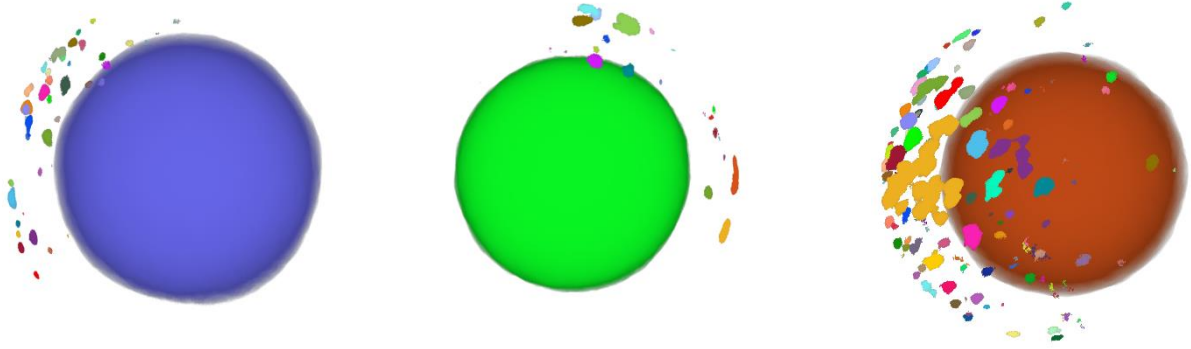
Particle C



Particle D

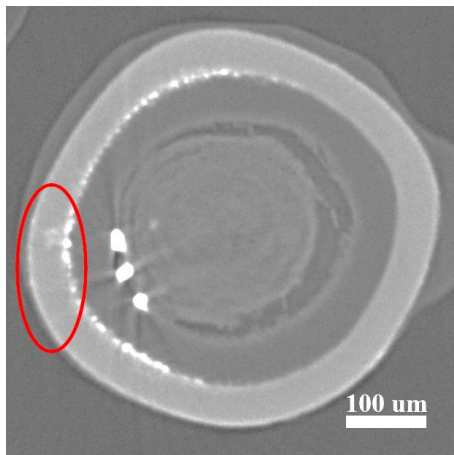


XCT - Particles A, C, and D



3D- renderings of dense features surrounding the kernels of Particles A, C, and D

- The dense features are primarily observed in large clusters along the IPyC side of the IPyC/Buffer interface where the two layers have separated. These features appeared to be nonuniformly distributed within particles.

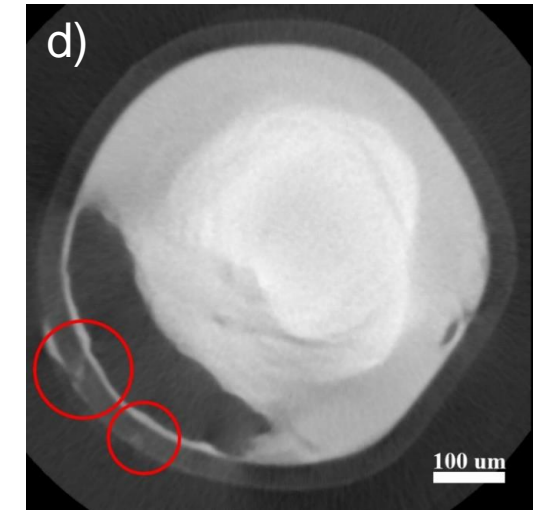
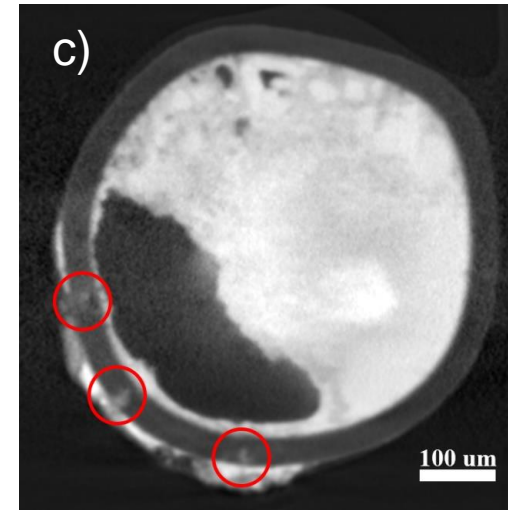
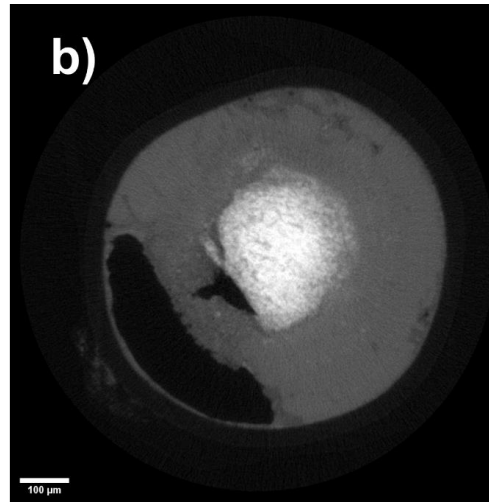
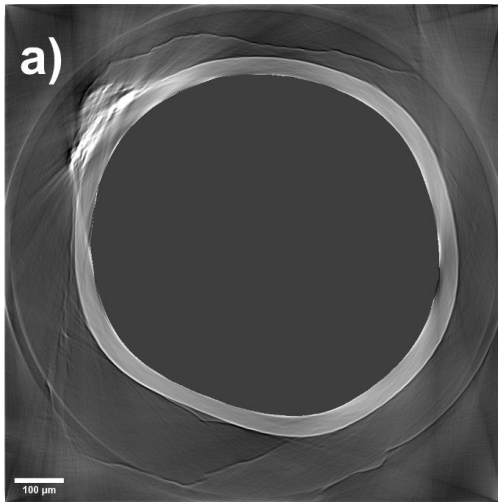


Particle C

- A lot of materials deposited on the SiC/IPyC interface.
- A small quantities of material deposited on the SiC exterior surface (circled in red).

XCT – Particle B

Particle B: no buffer nor IPyC



- Low energy (a) and high energy (b) XCT scans through the particle center, indicating no evidence of buffer nor IPyC. Dense material appeared dispersed throughout the interior of the SiC layer.
- (c) and (d) shows several locations on the SiC exterior surface where the unknown material appears to penetrate into the SiC layer.
- May be an example of a particle originally located near the Compact 1-7-9 surface attacked by nickel.

Characterization of Particles from AGR-5/6/7 Capsule 1

Preliminary SEM/EDS Analysis

Collaborators:

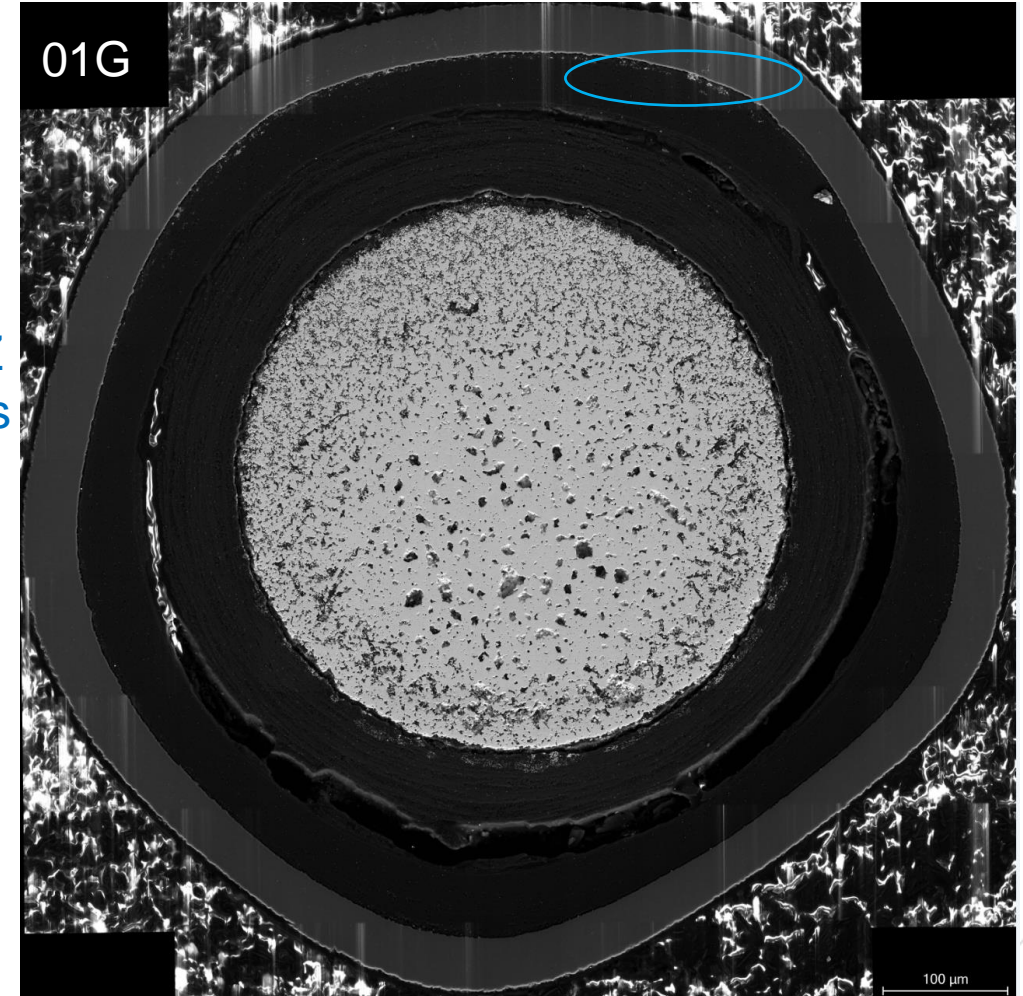
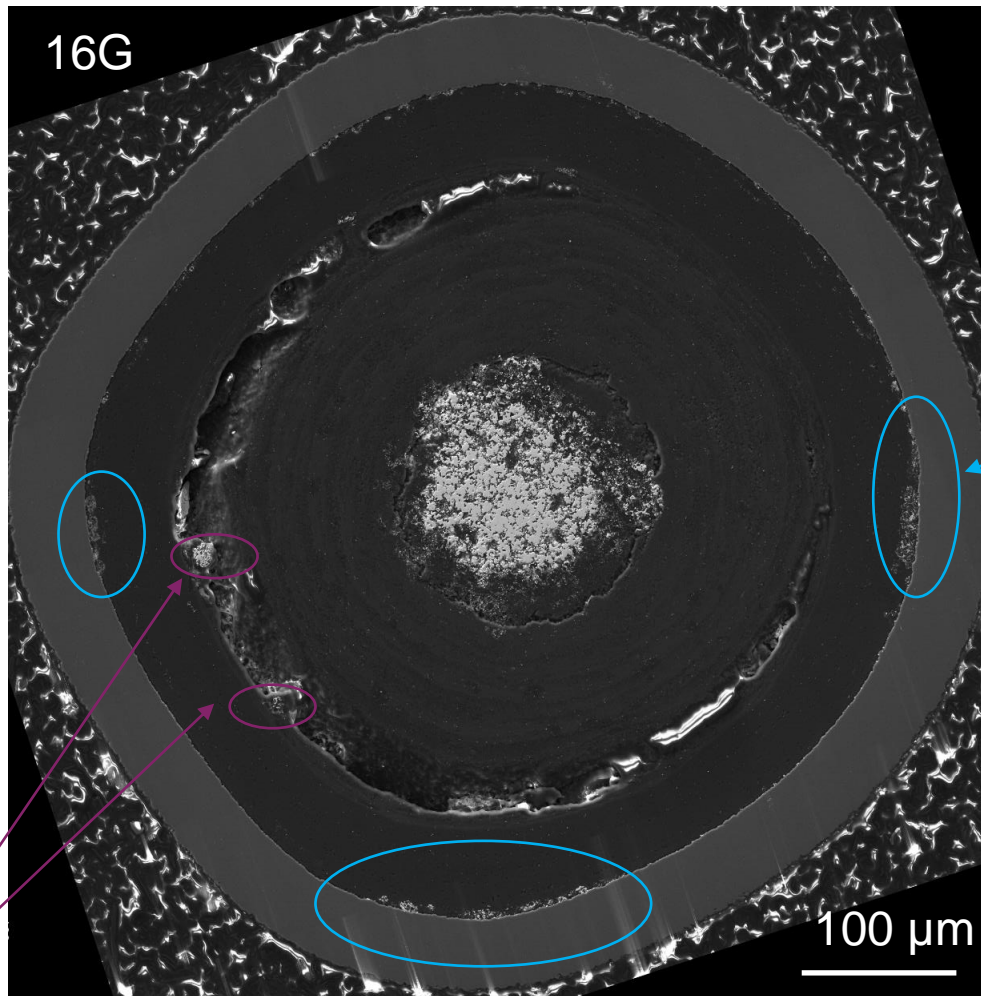
John D. Stempien

Rafael H. Garcia

Daniel J. Murray

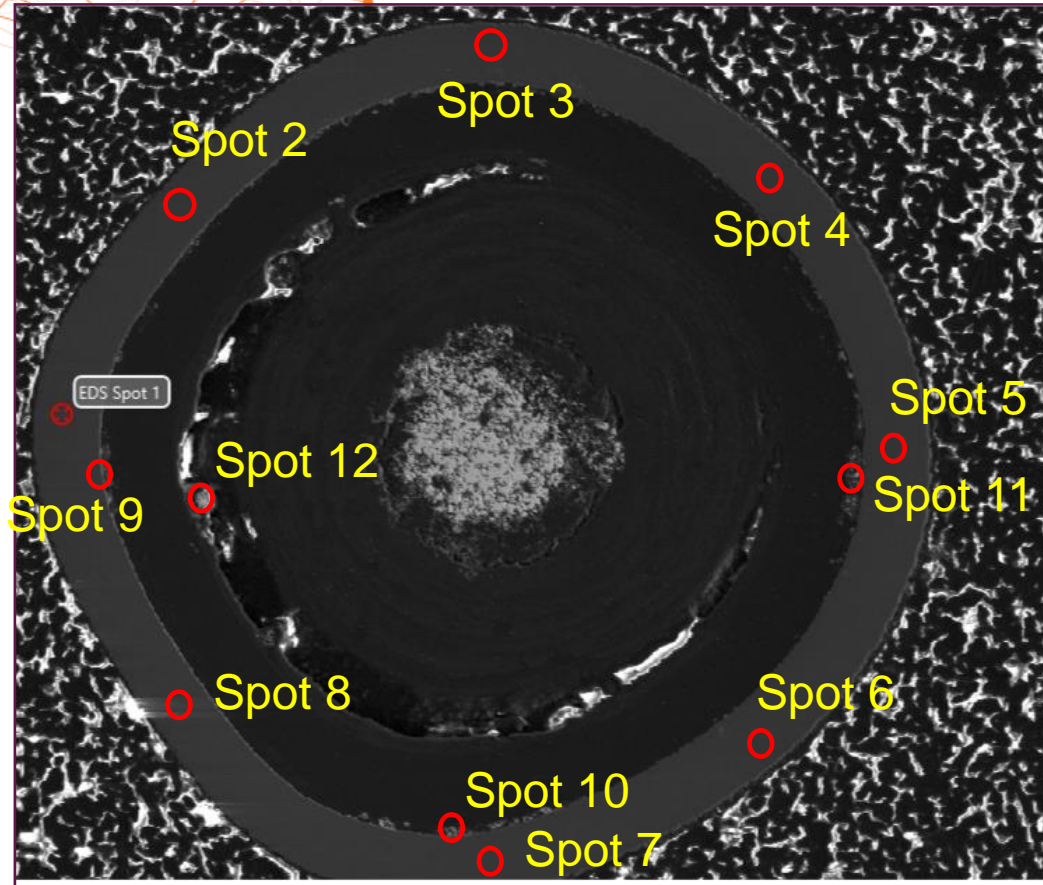
Fei Teng

MNT-16G and MNT-01G (Compact 1-7-9)



High Z materials were also observed at the IPyC side of the IPyC/Buffer interface where the two layers have separated, consistent with the XCT observation.

MNT-16G (Compact 1-7-9)

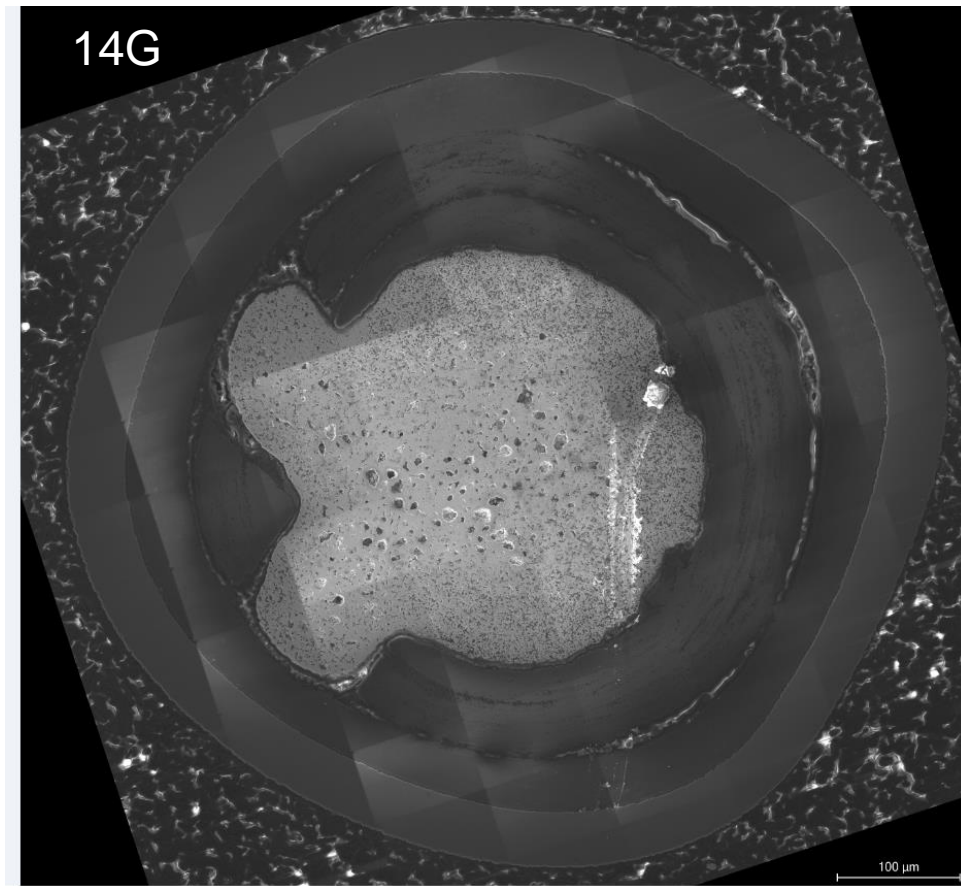
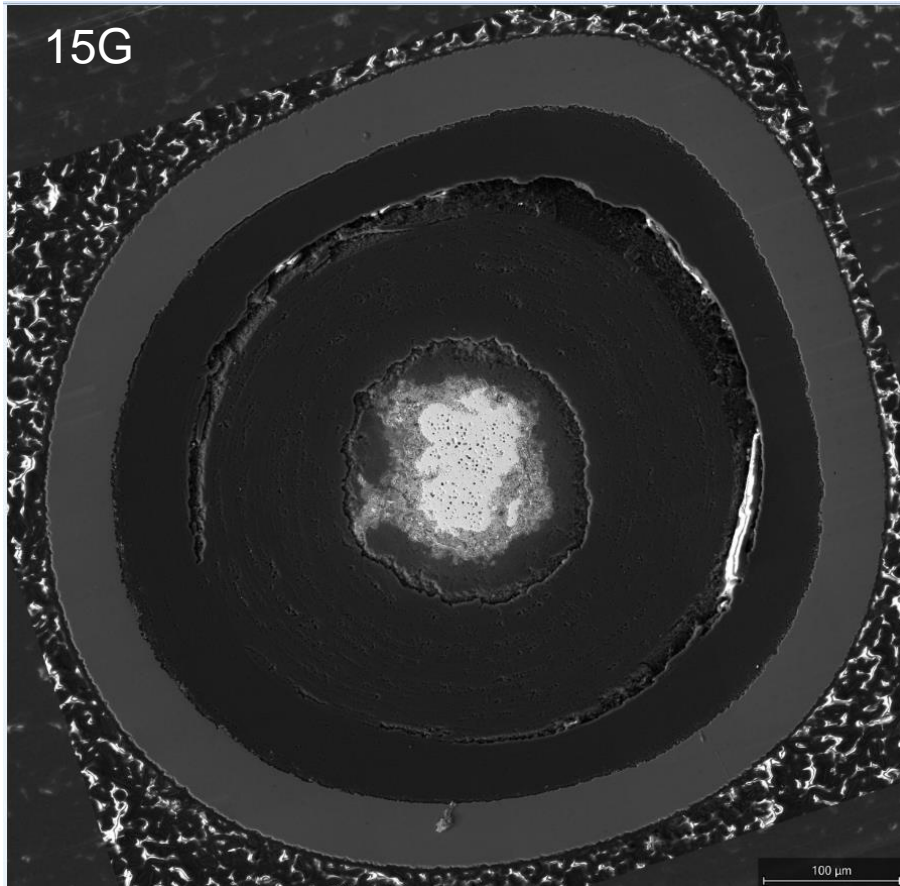


Spot	Location	Ni (wt%)
1	SiC	0.9
2	SiC	N/A
3	SiC	0.3
4	SiC	0.5
5	SiC	N/A
6	SiC	N/A
7	SiC	N/A
8	SiC	N/A
9	SiC/lpyC	2.6
10	SiC/lpyC	7.7
11	SiC/lpyC	12.4
12	lpyC/gap	N/A

Ni is detected in some parts of the SiC layer as well as on the fission product deposits between SiC and IPyC interface.

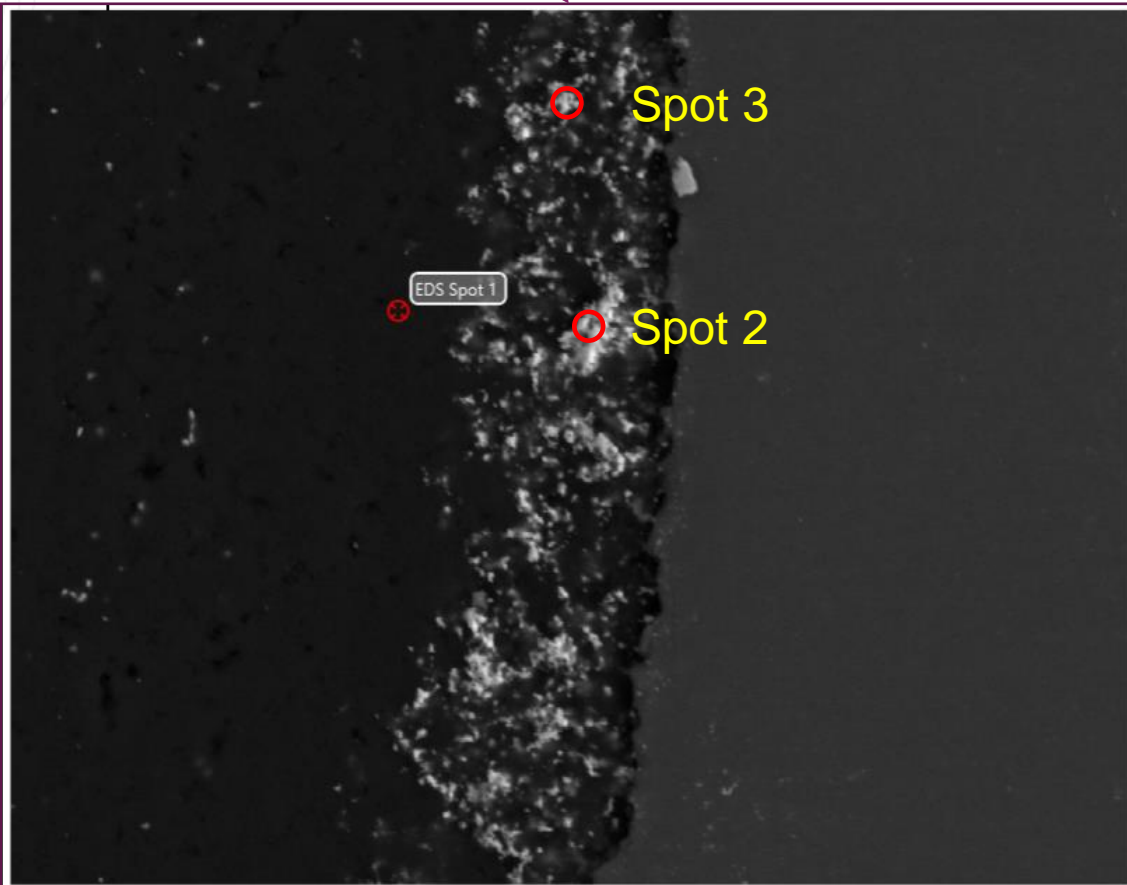
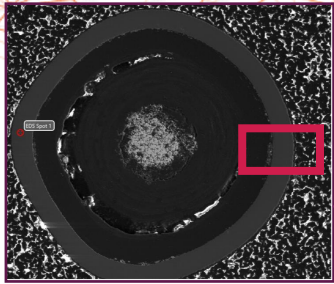
Note: Ni percentage is semi-quantitative. Si has much strong EDS peaks than C.

Particles from Compact 1-7-4

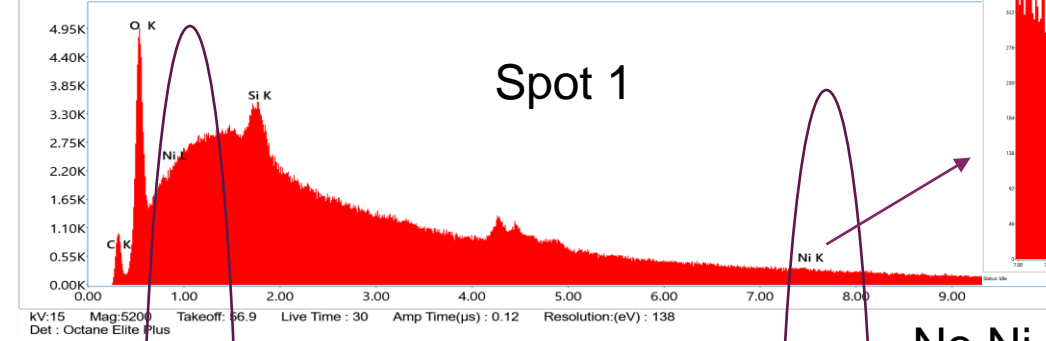


- Visibly less high Z materials deposits at SiC/IPyC
- No detection of Nickel

MNT-16G (Compact 1-7-9)

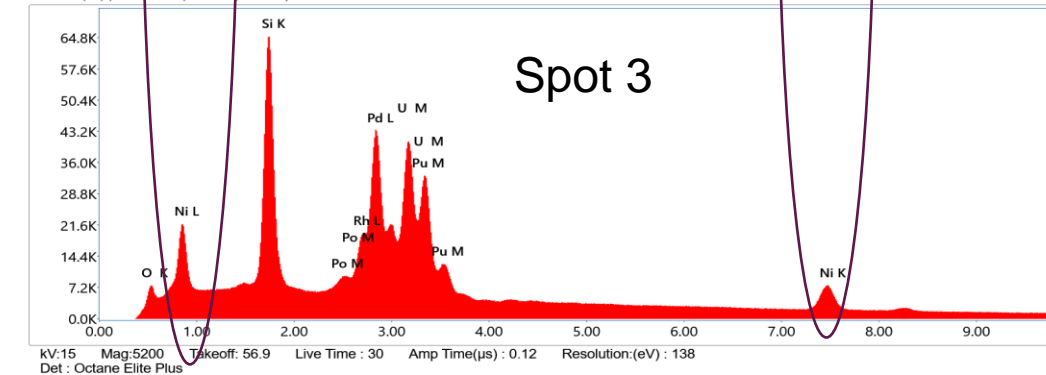
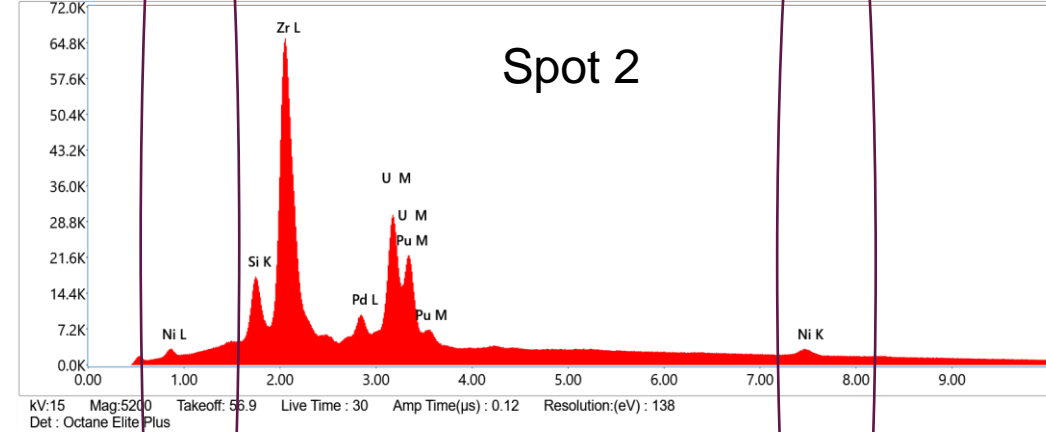


MNT-G (all) | MNT-16G | Area 2 | EDS Spot 1

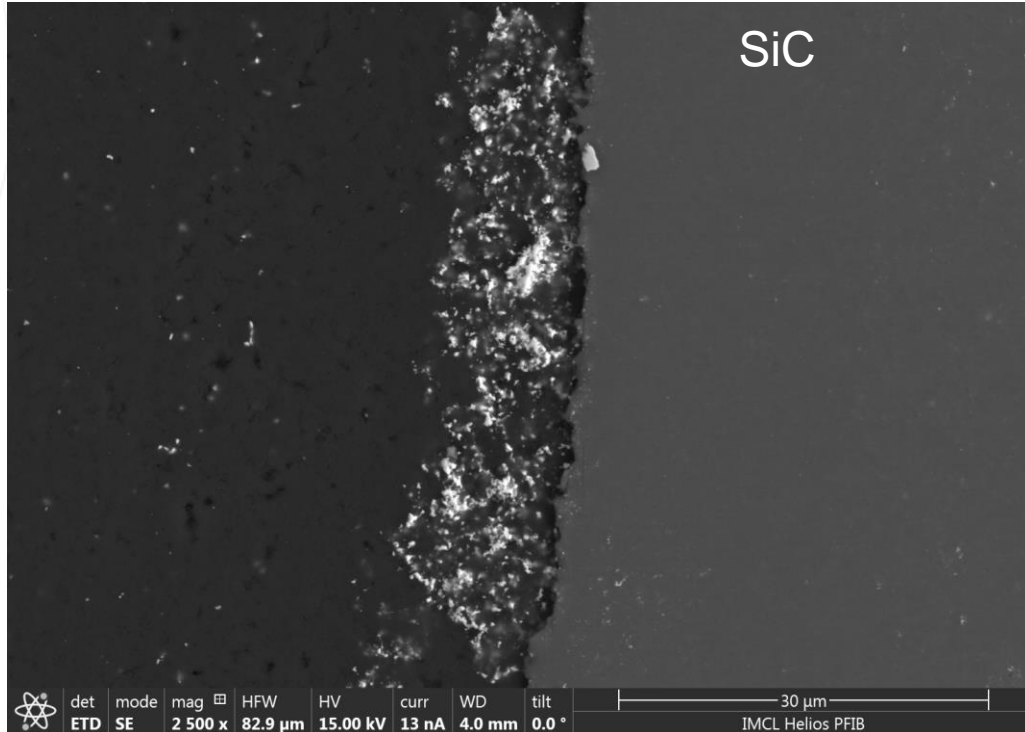


No Ni peak at Spot 1.

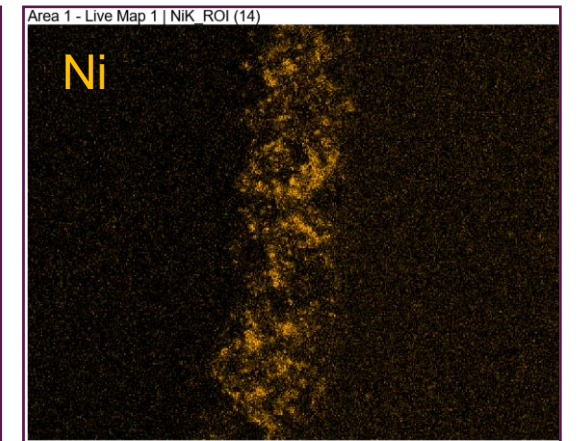
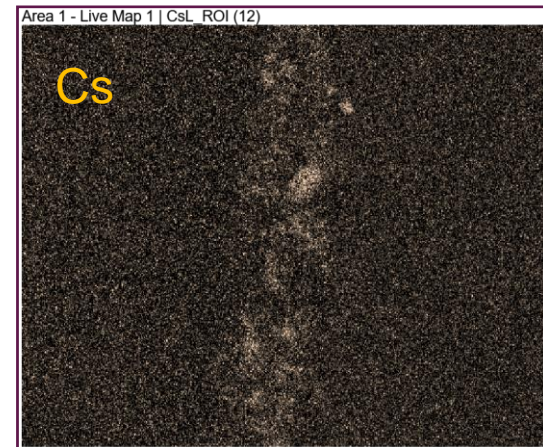
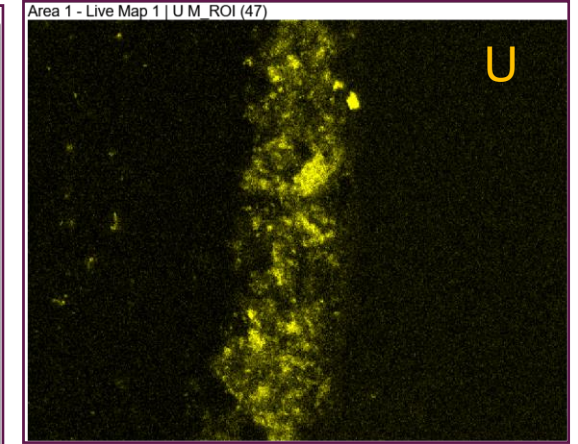
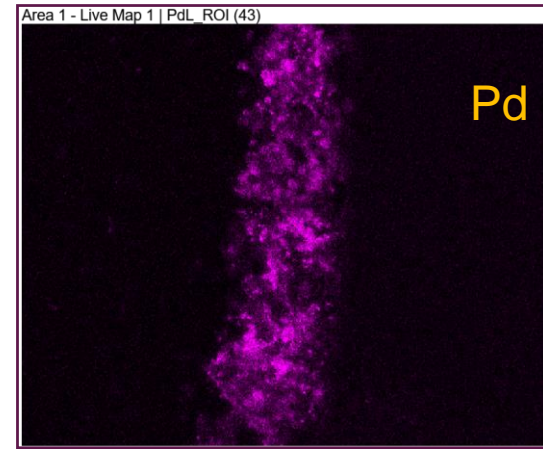
MNT-G (all) | MNT-16G | Area 2 | EDS Spot 2



MNT-16G (Compact 1-7-9)

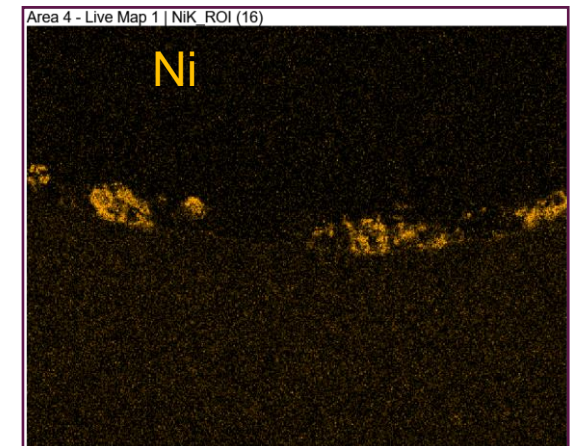
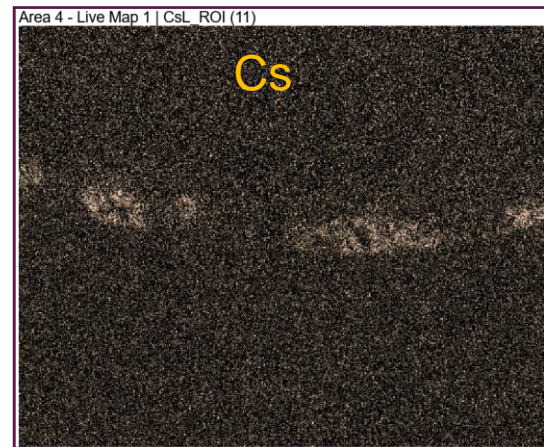
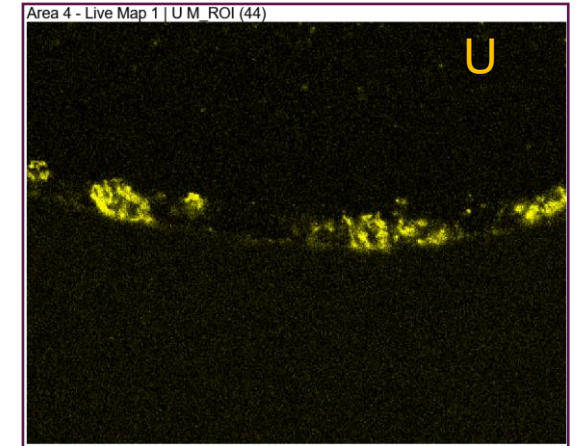
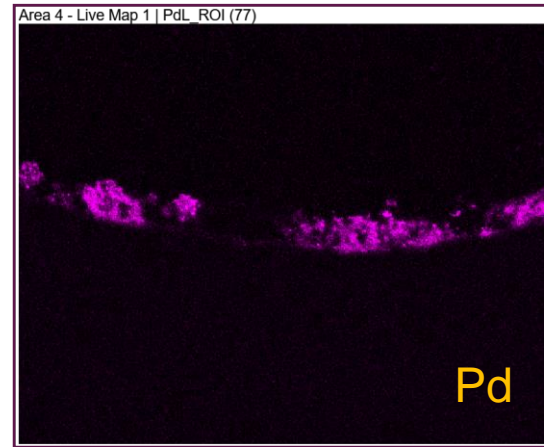
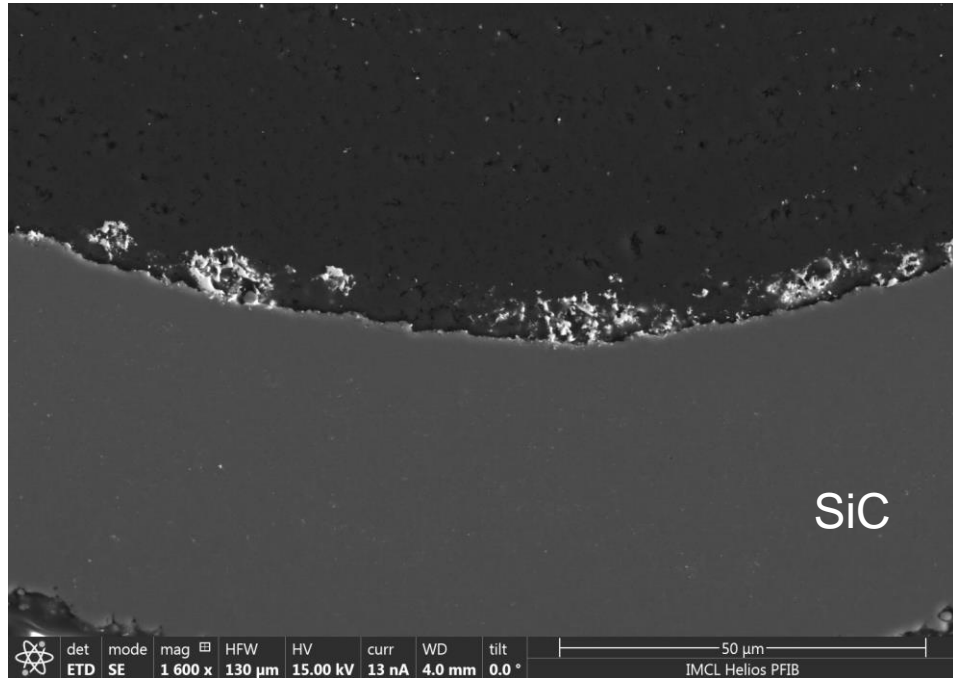
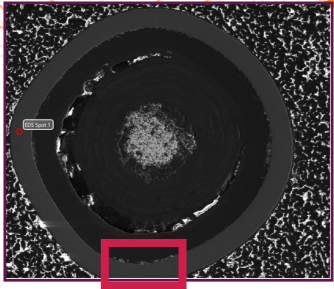


Fission products accumulated at the interface of SiC/IPyC. Ni is detected in these fission products.



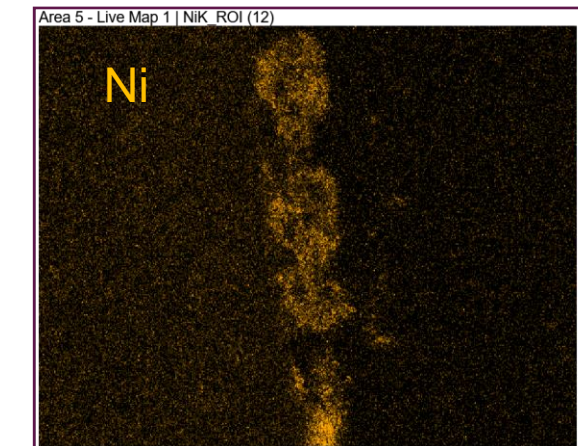
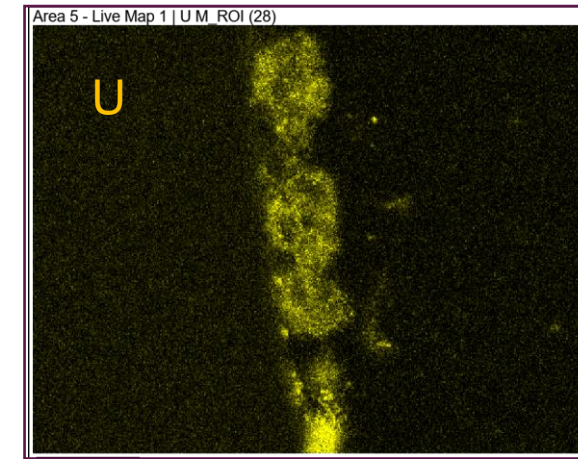
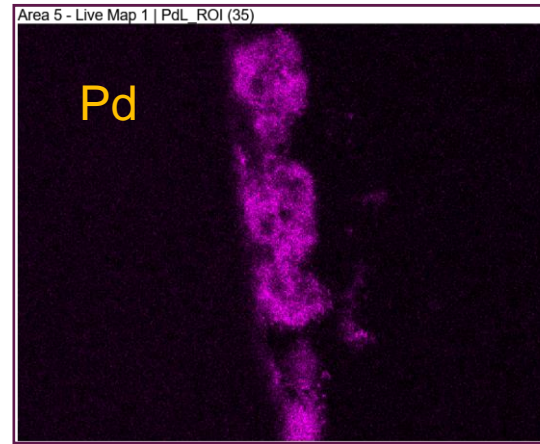
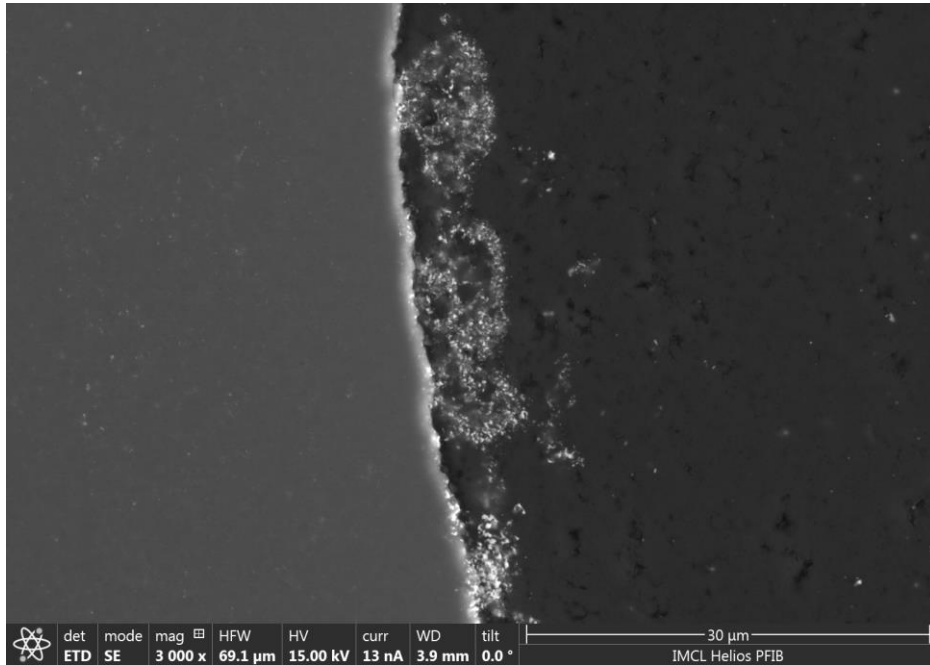
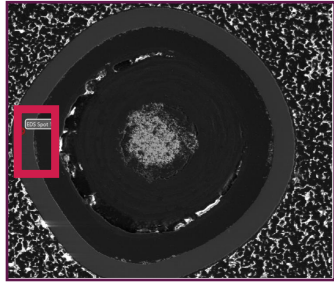
Element	Weight %	Error %
O K	1.7	10.8
Si K	69.5	3.9
Ni K	1.2	6.2
Pd L	5.7	4.8
Ag L	0.4	15.8
Cs L	2.3	4.4
U M	4.1	4.7
Pu M	7.5	4.1

MNT-16G (Compact 1-7-9)



Element	Weight %	Error %
O K	1.9	10.5
Si K	81.9	3.6
Ni K	0.8	9.2
Pd L	3.3	5.1
Cs L	2.1	5.2
Ce L	0.9	11.5
U M	2.9	4.3
Pu M	6.3	4.3

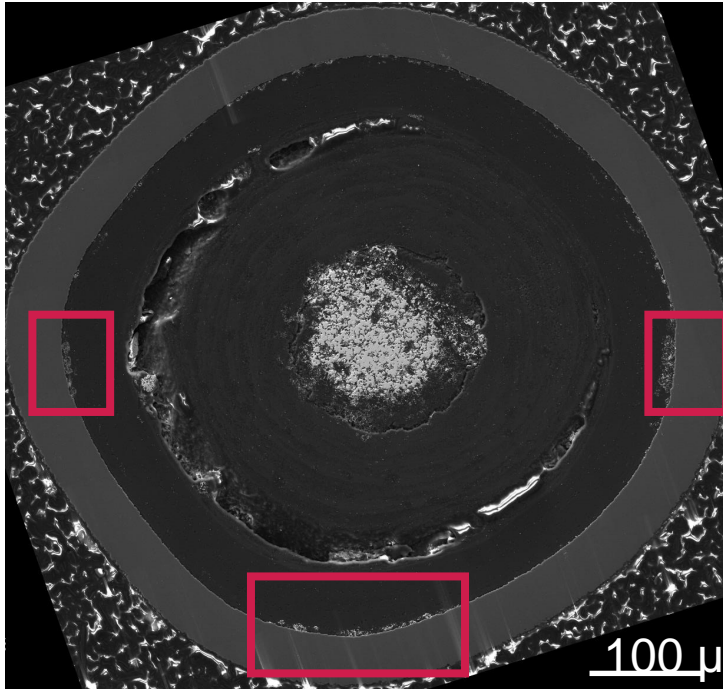
MNT-16G (Compact 1-7-9)



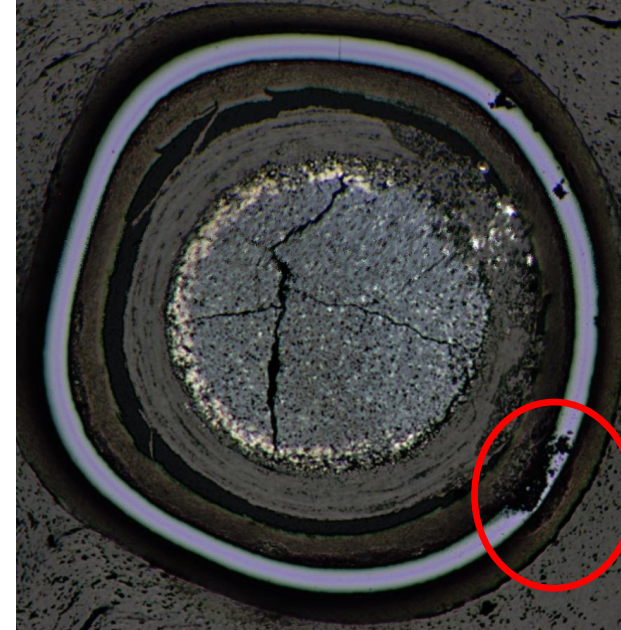
Element	Weight %	Error %
O K	2.6	10.1
Si K	71.9	3.9
Ni K	1.0	5.6
Pd L	4.8	4.8
Ce L	2.5	4.5
U M	3.4	4.4
Pu M	6.5	4.1

Nickel inside the particle

MNT-16G (Compact 1-7-9)



Particle from Compact 1-6-9

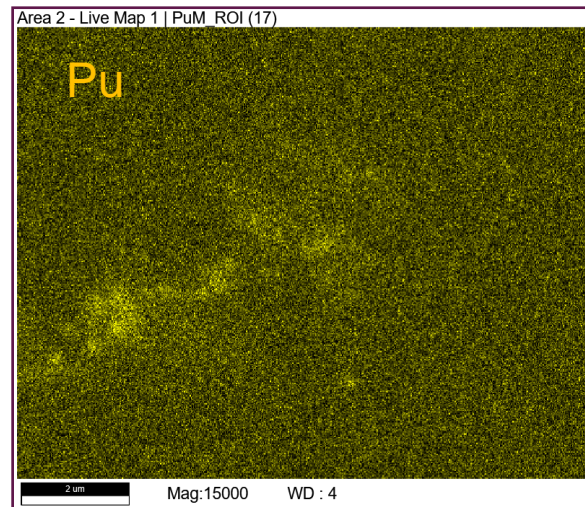
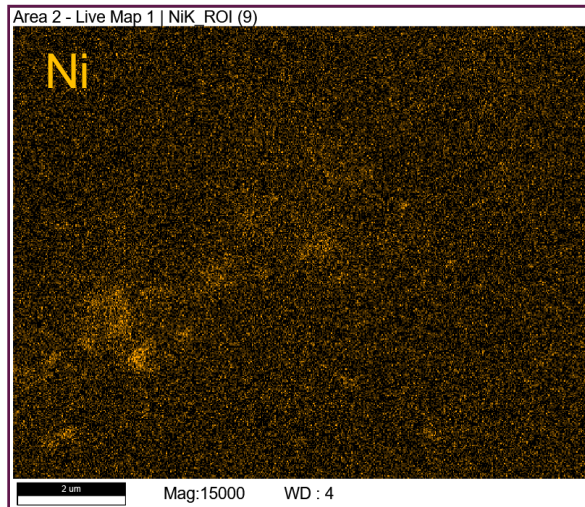
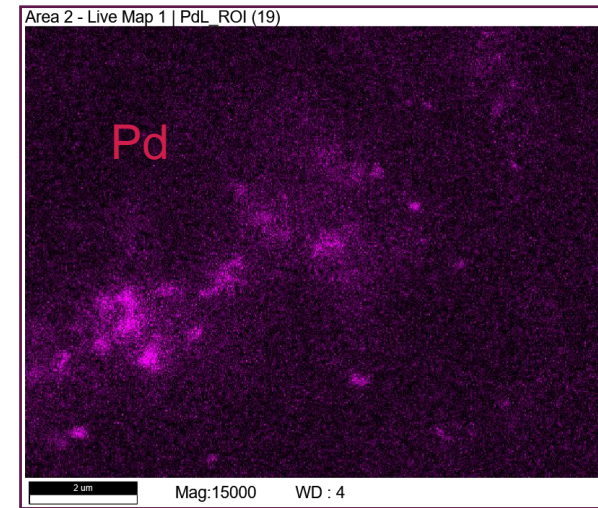
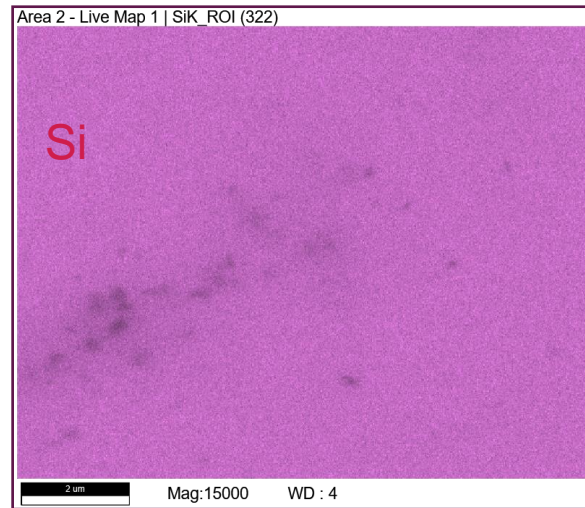
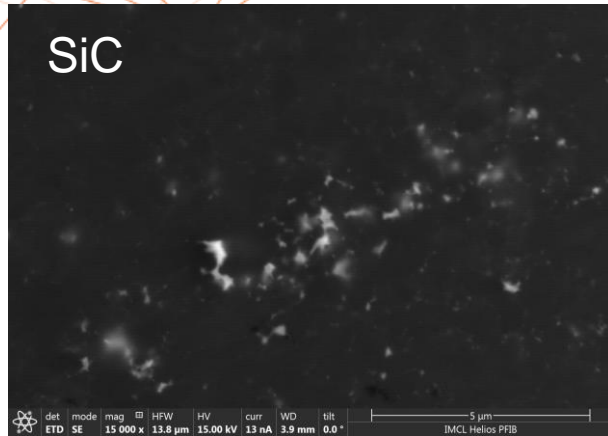


Looks like the
nickel attack
from inside out
→ Ni
penetrated
from another
plane

Nickel appears inside the particle with the cluster of fission products.

- is Ni penetrated the SiC in some other plane that we can't see here?
- Or is Ni diffusing through the SiC and then accumulating the locations?

MNT-01G (Compact 1-7-9) – Nickel on SiC



Element	Weight %	Error %
Si K	85.5	3.4
Ni K	0.4	9.9
Pd L	1.0	7.1
Cs L	0.5	10.9
Ce L	0.4	11.6
U M	1.1	6.0
Pu M	7.2	4.0

Fission products with Ni were observed on SiC.

Summary on Capsule 1 Particle Characterization

- SiC degradation was observed in Particle B with XCT. Non-uniform dense features were observed in large clusters along the IPyC side of the IPyC/Buffer interface where the two layers have separated in the other three particles.
- SEM/EDS results confirmed the presence of nickel in the SiC layer co-located with fission products along SiC/IPyC interface. This finding supports the hypothesis that particle failures were caused by the overheated thermocouples.
- We are currently working on characterizing the cross-section of Compact 1-6-9 with SEM EDS to observe evidence of nickel in the fuel matrix.

Thermal Conductivity of AGR-2 Particles

Collaborators:

John D. Stempien

Ethan Hisle

Amey Khanolkar

Tsvetoslav Pavlov

Subhashish Meher

Background and Motivation – Thermal Conductivity

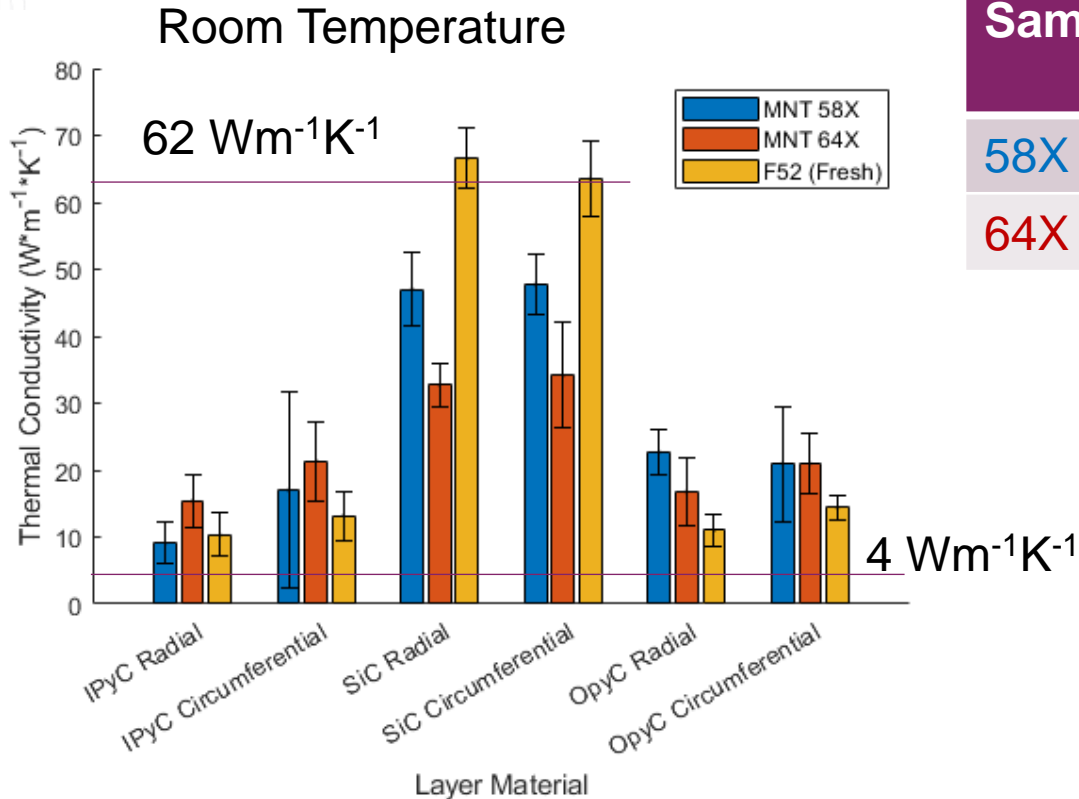
- Measurements of thermophysical properties are used in thermomechanical fuel performance code to model the fuel performance in normal and abnormal conditions. In PARFUME:

- Thermal conductivity of SiC:

$$k = \frac{17885}{T+273} + 2 \quad \text{W/(m}\cdot\text{K)}, T \text{ in } ^\circ\text{C}$$

- Thermal conductivity of IPyC and OPyC: $4 \text{ Wm}^{-1}\text{K}^{-1}$
- The sensitivity study (INL/EXT-18-44631) shows that variations of the thermal conductivity in each layer have negligible impact on the probability of SiC failure.
- This study uses a thermal conductivity microscope (TCM) to provide microscale measurements of thermal diffusivity and thermal conductivity. The objectives are to evaluate:
 - Accuracy of the values used in the models
 - How irradiation impacts the thermal conductivity

Results – Thermal Conductivity



Irradiated Sample	Compact (AGR-2)	TAVA temperature (°C)	Burnup (% FIMA)	Fluence (10 ²⁵ n/m ² E>0.18 MeV)
58X	2-4-3	1216	11.52	3.08
64X	5-1-3	1078	11.09	3.03

- The SiC thermal conductivity from the fresh fuel matches well with that in PARFUME.
- IPyC and OPyC have a 25 to 50% **increase** in thermal conductivity after irradiation. Layers appear to densify which may improve thermal transport.
- SiC thermal conductivity **decreases** *at least* 30 – 50% post irradiation depending on compact which is in line with presence of irradiation induced defects.



Summary – Thermal Conductivity

- OPyC and IPyC thermal conductivity increases with irradiation.
- SiC thermal conductivity decreases with irradiation.
- The changes in both instances are small relative to the ranges for these properties used in the PARFUME sensitivity study.



Idaho National Laboratory

Battelle Energy Alliance manages INL for the U.S. Department of Energy's Office of Nuclear Energy. INL is the nation's center for nuclear energy research and development, and also performs research in each of DOE's strategic goal areas: energy, national security, science and the environment.

WWW.INL.GOV